Journal of Geriatric Cardiology | JGC
RESEARCH ARTICLE
J Geriatr Cardiol 2021; 18(6): 426–439

Downregulation of miR-181a-5p alleviates oxidative stress and inflammation in coronary microembolization-induced myocardial damage by directly targeting XIAP

You ZHOU[1,*], Man-Yun LONG[1,*], Zhi-Qing CHEN[1], Jun-Wen HUANG[1], Zhen-Bai QIN[1], Lang LI[1,2,✉]

1. Department of Cardiology, the First Affiliated Hospital of Guangxi Medical University, Nanning, China; 2. Guangxi Key Laboratory of Precision Medicine in Cardio-cerebrovascular Diseases Control and Prevention, Nanning, China
[*]The authors contributed equally to this manuscript
✉ Correspondence to: drlilang1968@126.com
https://doi.org/10.11909/j.issn.1671-5411.2021.06.007

ABSTRACT

BACKGROUND Coronary microembolization (CME) is a complicated problem that commonly arises in the context of coronary angioplasty. MicroRNAs play crucial roles in cardiovascular diseases. However, the role and mechanism of miR-181a-5p in CME-induced myocardial injury remains unclear.

METHODS We established CME rat models. Cardiac function was detected by echocardiography. Haematoxylin-basic fuchsin-picric acid staining was used to measure micro-infarction size. Serum samples and cell culture supernatants were evaluated via enzyme-linked immunosorbent assay. Cellular reactive oxygen species were determined by dichloro-dihydro-fluorescein diacetate assay, and the other oxidative stress related parameters were assayed by spectrophotometry. The dual-luciferase reporter (DLR) assay and RNA pulldown were conducted to validate the association between miR-181a-5p and X-linked inhibitor of apoptosis protein (XIAP). The expression of miR-181a-5p and XIAP mRNA were determined by quantitative reverse transcription polymerase chain reaction. Proteins were evaluated via immunoblotting. The viability of the cell was evaluated via cell counting kit-8 assay.

RESULTS The miR-181a-5p level was significantly increased in CME myocardial tissues. Downregulation of miR-181a-5p improved CME-induced cardiac dysfunction and alleviated myocardial oxidative stress and inflammatory injury, whereas miR-181a-5p exhibited the opposite effects. Then, the DLR assay and RNA pulldown results revealed that miR-181a-5p directly targeting on XIAP. The XIAP level was found to be remarkably decreased after CME. XIAP overexpression attenuated CME-induced myocardial oxidative stress and inflammatory injury. Finally, *in vitro* rescue experiments revealed that knockdown of XIAP could abolish the protective effects of miR-181a-5p knockdown on hypoxia-induced cardiomyocyte oxidative stress and inflammatory injury.

CONCLUSIONS Downregulation of miR-181a-5p alleviates CME-induced myocardial damage by suppressing myocardial oxidative stress and inflammation through directly targeting XIAP.

Coronary microembolization (CME) is a coronary micro-circulation embolism and myocardial microinfarction caused by spontaneous rupture of coronary atherosclerotic plaques or micro-emboli during percutaneous coronary intervention (PCI) therapy.[1,2] The incidence of CME during perioperative PCI has been reported as 15%–20% and is up to 45% in high-risk patients.[3] The transient "no blood flow" or "slow blood flow" caused by CME is an independent predictor of long-term poor prognosis in patients with acute coronary syndrome.[4,5] Furthermore, CME can also lead to progressive myocardial malfunction, such as myocardial infarction, heart failure, arrhythmias, and reduction of coronary flow reserve fraction.[6–8] The mechanism underlying CME is extremely complex. Studies have reported that localized myocardial inflammation acts as a pivotal role in CME-induced myocardial injury, inhibition of tumor necrosis factor-α (TNF-α) improves CME-induced

cardiac dysfunction and alleviates myocardial necrosis.[9,10] Su, *et al*.[11] found that myocardial oxidative stress following CME plays a crucial role in CME-induced myocardial injury. Though there are advantages in both basic and clinical research for CME-induced myocardial damage, the underlying molecular mechanisms for CME are still unclear.

MicroRNAs (miRNAs), small non-coding single-stranded RNA molecules, have emerged as key regulators of gene expression at the post-transcriptional level by inhibiting mRNA translation and/or promoting mRNA degradation.[12] MiRNAs play crucial roles in various physiological and pathological processes such as oxidative stress, apoptosis, and various aspects of inflammation.[13,14] Numerous miRNAs were reported to involve in cardiovascular diseases.[15] For instance, overexpression of miRNA-129-5p protects against cardiomyocyte hypertrophy and heart failure.[16] MiR-708-3p alleviates inflammation and myocardial injury after myocardial infarction in mice.[17] Our previous studies also confirmed that miR-142-3p and miR-486-5p are involved in CME-induced myocardial injury.[18,19] Several studies have reported that miR-181 family plays a role in regulating vascular inflammation and immunity.[20] However, the functional and molecular mechanisms of miR-181a-5p in CME-induced myocardial injury are still unknown.

Hence, this study herein built a rat CME model by infusing microembolization spheres into the coronary artery. Results demonstrated that pre-treatment with miR-181a-5p antagomiR before CME modeling significantly improved cardiac functions and reduced micro-infarction size, while markedly alleviated oxidative stress and inflammation in the myocardial tissue. Whereas pre-treatment with miR-181a-5p agomiR before CME modeling exhibited the opposite effects. Additionally, X-linked inhibitor of apoptosis protein (XIAP) was identified as a direct target of miR-181a-5p. Finally, *in vitro* rescue experiments revealed that knockdown of XIAP could abolish the protective effects of miR-181a-5p knockdown on hypoxia-induced cardiomyocyte oxidative stress and inflammatory injury. Collectively, our data provided strong evidence that miR-181a-5p controls CME-induced myocardial injury via regulating XIAP. Knockdown of miR-181a-5p might act as a protective strategy for treating CME-induced myocardial injury.

MATERIALS AND METHODS

Animal Modeling and Grouping

The *in vivo* studies were based on suggested procedures of the US National Institutes of Health, and the approval for this study (No.201904019) was provided by the Animal Care and Use Committee of Guangxi Medical University, China. Male Sprague-Dawley rats (150) having body weight of about 250−300 g were used. The controlled humidity of 50%−60% and temperature of 23 ± 2 °C were maintained. Food and water were provided to rats in a fully maintained environment of 12:12 h light and dark period. CME model was established by the underlined process. Pentobarbital hydrochloride (Hongyun Long Biological Technology, Wuhan, China) of 30−40 mg/kg was provided by an intraperitoneal injection under anesthesia, followed by tracheotomy and intubation. A minute animal ventilator (AlcBio, Shanghai, China) was employed to facilitate respiration. The chest was exposed between the 3rd and 4th ribs in the left side of the sternum, followed by the separation of the upward arch region (ascending aorta) and clamped via vascular clamp for 10 s. Then micro injector (Beilunhe Medical Industry, Nanning, China) was used for injecting 3,000 plastic microspheres (diameter: 42 μm; Biosphere Medical Inc., Rockland) from the apex of the left ventricle. Then the chest was closed while the trachea cannula was removed post steady breathing. The penicillin (dose: 80,000 units; PhytoTech, Kansas, USA) was given intraperitoneally. Similar surgery was conducted via injecting normal saline (Yuntai Technology, Shanghai, China) to the Sham group. As our previous study has confirmed that the cardiac function reached the worst value at 9 h after CME,[21] the blood and heart samples were collected from the Sham group as well as the CME group at 9 h after modeling. Heart samples were taken from the left ventricular near the apex in all groups. The fixing of heart samples was carried out in paraformaldehyde (concentration: 4%; ServiceBio, Wuhan, China) or instantly kept in liquid nitrite for further analysis.

Adeno-associated Virus, Plasmids, AntagomiR and AgomiR Transfection

All adeno-associated virus (AAVs), plasmids, miR-181a-5p antagomiR and agomiR were gener-

ated via GeneChem (Shanghai, China). A total titer of 10^{11} TU (transducing units) AAV was diluted with 200 μL transfection reagents (Engreen Biosystem, Beijing, China), and a 100 μg of antagomiR or agomiR was diluted with 200 μL saline. Then the mixture was injected into the vein in the mice tail three weeks before modeling. The cells transfection was carried out with the XIAP-shRNA, miR-181a-5p antagomiR and agomiR. Lipofectamine™ 2000 (Life Technologies, USA) was used for transfection.

Detection of Cardiac Function

The underlined parameters were calculated [*i.e.*, left ventricular ejection fraction (LVEF)]. The 12 MHz was the probe frequency. The obtained values were the mean of three-cardiac cycles. Echocardiographic results were calculated and evaluated via blinding to various therapies.

Measurement of Myocardial Micro-infarction Size

The red-stained section (ischemia or necrotic) evaluation was carried out via a DMR-Q550 pathological picture analyzer (Lei, Germany). The five vision fields (× 200 magnification) were randomly chosen from individual haematoxylin-basic fuchsin-picric acid (HBFP) staining sections for evaluation of the infarction area via plane procedure with Leica Qwin analysis software (Leica Microsystems Inc., Buffalo Grove, Illinois).

Enzyme-linked Immunosorbent Assay

The concentration of cardiac troponin I (cTnI) and lactate dehydrogenase (LDH) in serum samples or cell culture supernatants were assayed via enzyme-linked immunosorbent assay (ELISA) kits (R&D Systems, USA) as suggested by the manufacturer.

Measurement of Reactive Oxygen Species Generation

Intracellular reactive oxygen species (ROS) level was assayed by the dichloro-dihydro-fluorescein diacetate (DCFH-DA) (Sigma, USA). After the introduction of different stimulus, samples were incubated with 50 μM DCFH-DA at 37 °C for 30 min in the dark. Then, the samples were washed twice using cold phosphate buffered saline (ServiceBio, Wuhan, China). The fluorescence images of intracellular ROS were acquired by using fluorescence microscopy (Olympus IX51, Japan). The average fluorescence intensity was analyzed by using the image analysis system (ImageJ, National Institutes of Health).

Biochemical Analysis

The levels of malondialdehyde (MDA), superoxide dismutase (SOD), glutathione (GSH) and catalase enzymes (CAT) in myocardium or H9c2 cells were determined spectrophotometrically using assay kits (Nanjing Jiancheng Bioengineering Research Institute, Nanjing, China) and were normalized to homogenate protein levels that were measured using a bicinchoninic acid protein assay kit (Solarbio, Beijing, China).

RNA Isolation and Quantitative Polymerase Chain Reaction Analysis

The total RNA was extracted from left ventricle myocardium as suggested by the manufacturer via TRIzol (Invitrogen, CA, USA). The RNA concentration was evaluated via NanoDrop (Thermo Scientific, USA). cDNA was synthesized with the help of a reverse transcription kit (TaKaRa, Japan). The obtained products of polymerase chain reaction were evaluated via SYBR-Green I (Sangon Biotech, Shanghai, China). The relative gene expression was identified via $2^{-\Delta\Delta CT}$ formula. The gene specific primers were as follows: miR-181a-5p primers: 5′-CAACATTCAACGCTGTCGGTGAGT-3′, downstream: 5′-CGCTTCACGAATTTGCGTGTCAT-3′; XIAP primers: upstream: 5′-TCGGGCTGCATAATGAGGACTG-3′, downstream: 5′-CCTTTTCGCGCCAAGCAATC-3′; U6 primers: upstream: 5′-GCTTCGGCAGCACATATACTAAAAT-3′, downstream: 5′-CGCTTCACGAATTTGCGTGTCAT-3′; and glyceraldehyde 3-phosphate dehydrogenase (GAPDH) primers: upstream: 5′-GGAAACCCATCACCATCTTC-3′, downstream: 5′-GTGGTTCACACCCATCACAA-3′.

Immunoblotting

The total of myocardium proteins were extracted via 10% to 15% SDS-PAGE (Sangon Biotech, Shanghai, China) and transformed onto polyvinylidene fluoride membranes (Merck Millipore, Germany). The skimmed milk (concentration: 5%; Sangon Biotech, Shanghai, China) was used for the blockage of the

membrane for 60 min at 25 °C. Then the membrane incubation was carried out with primary antibodies at 4 °C for 24 h. The primary antibodies specific to XIAP (Cat. No.ab229050, 1:1,000), TNF-α (Cat. No.ab205587, 1:1,000), interleukin-1β (IL-1β; Cat. No.ab254360, 1:1,000), interleukin 6 (IL-6; Cat. No.ab9324, 1:1,000) and GAPDH (Cat. No.ab9485, 1:10,000) were provided by Abcam (Cambridge, UK), followed by Tris-buffered saline with Tween-20 (TBST) washing thricely, the membrane incubation was carried out with secondary antibodies fused with horseradish peroxidase in TBST for 60 min at 25 °C. Enhanced chemiluminescence detection system (Santa Cruz, CA, USA) was considered for the identification of the signals. However, Image Lab (Bio-Rad, USA) software was used for the evaluation of protein bands.

Bioinformatics Analysis and Dual-luciferase Reporter Assay

The TargetScan software were employed to evaluate the potential binding sequences within the 3′ untranslated region of XIAP to miR-181a-5p. Site-Directed Mutagenesis kit (Strata gene, La Jolla, CA, USA) was used for the insertion of mutation into the candidate binding sequences. psiCHECK-2 vector (Promega, Madison, WI, USA) was used for cloning of the wild-type (WT) or mutant (MUT) binding sequences of XIAP and then co-transfected into primary cardiomyocytes with miR-181a-5p mimic or miR-NC via Lipofectamine 2000 (Life Technologies, USA), as suggested by the manufacturer and post two days, dual-luciferase reporter (DLR) activity was evaluated.

RNA Pulldown Assay

Cardiomyocytes transfection was performed with biotinylated miRNA. Post two days, cells were harvested. The incubation of cell lysates was conducted with the help of M-280 streptavidin magnetic beads (Invitrogen, CA, USA). To perform the quantitative reverse transcription polymerase chain reaction (qRT-PCR) analysis, TRIzol reagent (Invitrogen, CA, USA) was utilized for the purification of bounded RNAs.

Cell Culture and Treatment

H9c2 cell lines were provided by the American Type Culture Collection (ATCC; Rockville, MD, USA). The underlined cell lines were seeded in Dulbecco's modified Eagle's medium (DMEM; Corning Inc., NY, USA). Next, cells were then treated under normoxic (21% O_2) or hypoxic conditions (10% O_2), with cells cultured under hypoxic conditions being treated with miR-181a-5p antagomiR and/or XIAP-shRNA.

Cell Viability Assay

The total number of live cells was analyzed via the cell counting kit-8 (Dojindo, Japan). The cell counting kit-8 was employed according to the provided guidelines of the kit supplier.

Statistical Analysis

The SPSS 20.0 software (IBM Corporation, Armonk, NY, USA) was used for data analysis and calculate. The results were displayed as mean ± SE (standard error). Student's *t*-test was considered to assess the variations between two independent groups. For multiple groups, statistical differences were evaluated via one-way ANOVA followed by Bonferroni test. All the experiments were performed in triplicate. A two-sided *P*-value < 0.05 was considered statistically significant.

RESULTS

Upregulation of MiR-181a-5p in Heart Tissue of Rats

As described in the sections method, we established rat CME models. Hematoxylin and eosin staining showed inflammatory cell infiltration, disordered or ruptured myocardial fibers, and interstitial edema were visible surrounding microspheres in CME model animals (Figure 1A). Compared with the Sham group, the CME group showed a significant reduction in cardiac functions, as reflected by marked reductions of LVEF (Figure 1B). HBFP staining showed that the micro-infarction size was significantly increased in the CME group compared to the Sham group (Figure 1C). Meanwhile, the cTnI level was significantly higher in the CME group than the Sham group (Figure 1D). The ROS level in heart tissue was dramatically elevated in the CME group compared to the Sham group (Figure 1E). The MDA level was also significantly increased in

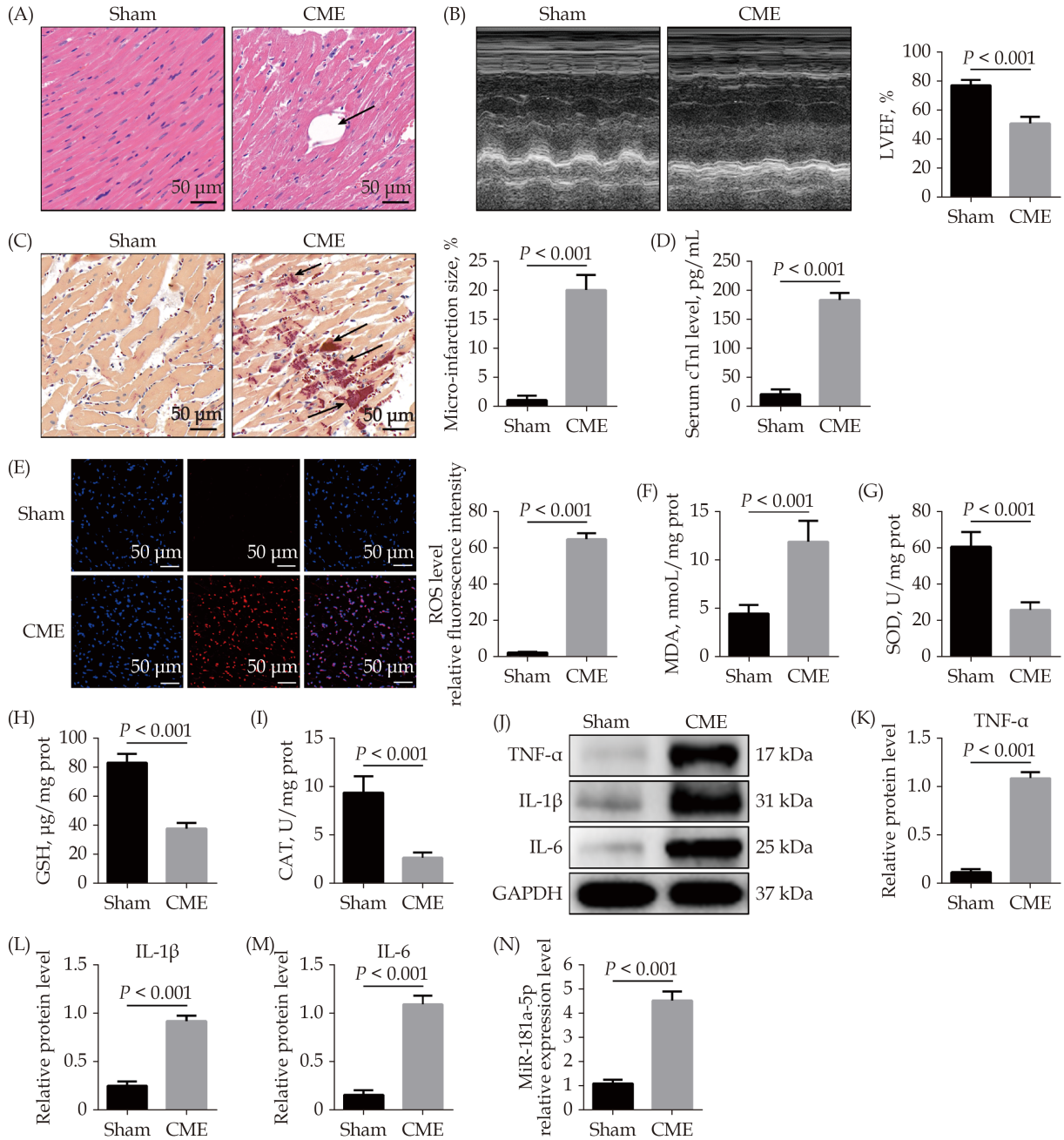

Figure 1 Upregulation of miR-181a-5p in heart tissue of rats. (A): Myocardial tissue samples stained with hematoxylin and eosin. Microspheres are marked using black arrows (× 200 magnification, scale bar = 50 μm); (B): echocardiography was used to assess cardiac function and to quantify LVEF (n = 10); (C): haematoxylin-basic fuchsin-picric acid staining was used to measure micro-infarction size (× 200 magnification, scale bar = 50 μm) (n = 6); (D): serum cTnI concentration in each group (n = 10); (E): the ROS production was detected by the dichloro-dihydro-fluorescein diacetate assay (× 200 magnification, scale bar = 50 μm) (n = 6); (F–I): myocardial MDA, SOD, GSH, and CAT level in each group (n = 6); (J–M): western blotting was used to quantify myocardial TNF-α, IL-1β, and IL-6 protein level, with glyceraldehyde 3-phosphate dehydrogenase as a loading control (n = 3); and (N): miR-181a-5p level was significantly elevated in heart tissue following CME (n = 10). Data were shown as mean ± SE (standard error) based on at least three independent experiments. CAT: catalase enzymes; CME: coronary microembolization; cTnI: cardiac troponin I; GSH: glutathione; IL-1β: interleukin-1β; IL-6: interleukin 6; LVEF: left ventricular ejection fraction; MDA: malondialdehyde; ROS: reactive oxygen species; SOD: superoxide dismutase; TNF-α: tumor necrosis factor-α.

the CME group compared to the Sham group (Figure 1F), but the activities of SOD, GSH and CAT attenuated considerably (Figure 1G–1I). Western blotting showed that pro-inflammatory cytokines such as TNF-α, IL-1β, and IL-6 in myocardial tissue were significantly increased after CME (Figure 1J–1M). The qRT-PCR results demonstrated a significant up-regulation in miR-181a-5p in the CME group (Figure 1N).

Downregulation of MiR-181a-5p Alleviates CME-induced Myocardial Oxidative Stress and Inflammatory Injury

To study the role of miR-181a-5p in CME-induced myocardial damage, we designed a miR-181a-5p antagomiR. The qRT-PCR results suggested that intervention of antagomiR decreased miR-181a-5p expression level significantly (Figure 2A). MiR-181a-5p antagomiR prominently improved CME-caused cardiac dysfunction (Figure 2B & 2C), while HBFP staining showed less micro-infarction area compared to the CME + anta-NC group (Figure 2D & 2E). Moreover, serum cTnI content was lower than in the CME + anta-NC group (Figure 2F). Downregulation of miR-181a-5p significantly reduced ROS and MDA level in heart tissue undergoing CME (Figure 2G–2I). On the contrary, antioxidant enzymes such as SOD, GSH, and CAT was increased significantly in the CME + anta-181 group compared to the CME + anta-NC group (Figure 2J–2L). Immunoblotting results revealed a considerable decrease in myocardial pro-inflammatory cytokines (TNF-α, IL-1β and IL-18) in the CME + anta-181 group than the CME + anta-NC group (Figure 2M & 2N). The underlined results indicated that downregulation of miR-181a-5p attenuated CME-caused myocardial oxidative stress and inflammatory injury.

Overexpression of MiR-181a-5p Aggravates CME-induced Myocardial Oxidative Stress and Inflammatory Injury

To further explore the effect of miR-142-3p on CME, we also performed gain-of-function experiments. The qRT-PCR results suggested that transfection with miR-181a-5p agomiR elevated miR-181a-5p expression level in myocardium significantly (Figure 3A). MiR-181a-5p agomiR prominently reduced LVEF after CME (Figure 3B & 3C), while HBFP staining showed larger micro-infarction area compared to the CME + ago-NC group (Figure 3D & 3E). Moreover, serum cTnI content was higher than in the CME + ago-NC group (Figure 3F). Overexpression of miR-181a-5p significantly increased ROS and MDA level in heart tissue following CME (Figure 3G–3I). On the contrary, SOD, GSH, and CAT level were reduced significantly in the CME + ago-181 group compared to the CME + ago-NC group (Figure 3J–3L). Immunoblotting results revealed that the expression level of TNF-α, IL-1β and IL-18 proteins in myocardium was increased significantly in the CME + anta-181 group compared to the CME + anta-NC group (Figure 3M & 3N). All these results suggested that overexpression of miR-181a-5p aggravated CME-caused myocardial oxidative stress and inflammatory injury.

Correlation of XIAP and MiR-181a-5p

The bioinformatics tools were employed for the prediction of miR-181a-5p target genes via TargetScan (http://www.targetscan.org/vert_72/). XIAP was evaluated as a candidate miR-181a-5p target (Figure 4A). MiR-181a-5p target gene XIAP, either at the gene or protein level, was considerably decreased in the CME group (Figure 4B & 4C). Next, XIAP was overexpressed by AAV-pcDNA3.1-XIAP but was silenced by AAV-shXIAP in myocardium (Figure 4D–4F). Further experiments showed that overexpression of XIAP significantly downregulated miR-181a-5p level and inhibition of XIAP remarkably upregulated miR-181a-5p level in heart tissue (Figure 4G). Moreover, it was observed that the expression of XIAP mRNA was significantly upregulated by miR-181a-5p knockdown and was remarkably downregulated via miR-181a-5p overexpression in heart tissue (Figure 4H). As shown in Figure 4I, the luciferase activity was considerably decreased when cells transfection was carried out with miR-181a-5p mimics in WT-XIAP. However, no significant difference was found in MUT-XIAP. Pulldown assay was performed and revealed that XIAP could only be pulled down via WT bio-labeled miR-181a-5p, but not the mutated oligos (Figure 4J). The underlined results revealed that miR-181a-5p directly targeting and negatively regulating XIAP.

Overexpression of XIAP Attenuates CME-caused Myocardial Oxidative Stress and Inflammatory Injury

To research the role of XIAP in CME, we performed gain-of-function experiments. The elevated expres-

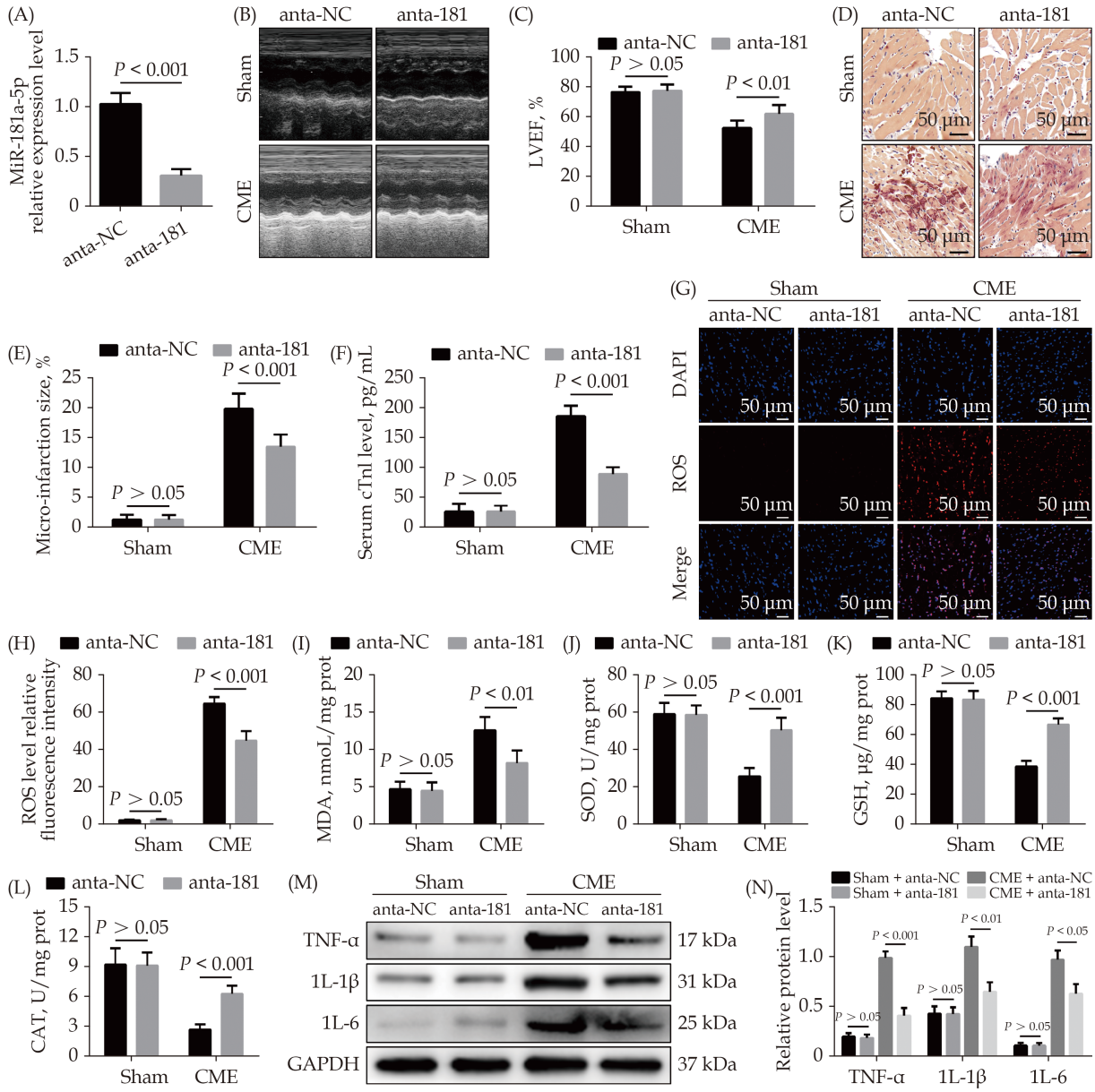

Figure 2 Downregulation of miR-181a-5p alleviates CME-induced myocardial oxidative stress and inflammatory injury. (A): Transfection with miR-181a-5p antagomiR decreased myocardial miR-181a-5p level significantly; (B & C): echocardiography was used to assess cardiac function and to quantify LVEF (n = 10); (D & E): haematoxylin-basic fuchsin-picric acid staining was used to measure micro-infarction size (× 200 magnification, scale bar = 50 μm) (n = 6); (F): serum cTnI concentration in each group (n = 10); (G & H): the ROS production was detected by the dichloro-dihydro-fluorescein diacetate assay (× 200 magnification, scale bar = 50 μm) (n = 6); (I–L): myocardial MDA, SOD, GSH, and CAT level in each group (n = 6); and (M & N): western blotting was used to quantify myocardial TNF-α, IL-1β, and IL-6 protein level, with glyceraldehyde 3-phosphate dehydrogenase as a loading control (n = 3). Data were shown as mean ± SE (standard error) based on at least three independent experiments. CAT: catalase enzymes; CME: coronary microembolization; cTnI: cardiac troponin I; GSH: glutathione; IL-1β: interleukin-1β; IL-6: interleukin 6; LVEF: left ventricular ejection fraction; MDA: malondialdehyde; ROS: reactive oxygen species; SOD: superoxide dismutase; TNF-α: tumor necrosis factor-α.

sion of XIAP significantly improved LVEF following CME (Figure 5A & 5B). The elevated expression of XIAP decreased micro-infarction size significantly (Figure 5C & 5D). Overexpression of XIAP decreased serum cTnI concentration following CME (Figure 5E). Transfection with Ad-XIAP remarkedly reducing myocardial ROS and MDA induced by CME (Figure 5F–5H), while dramatically elevating myocardial SOD,

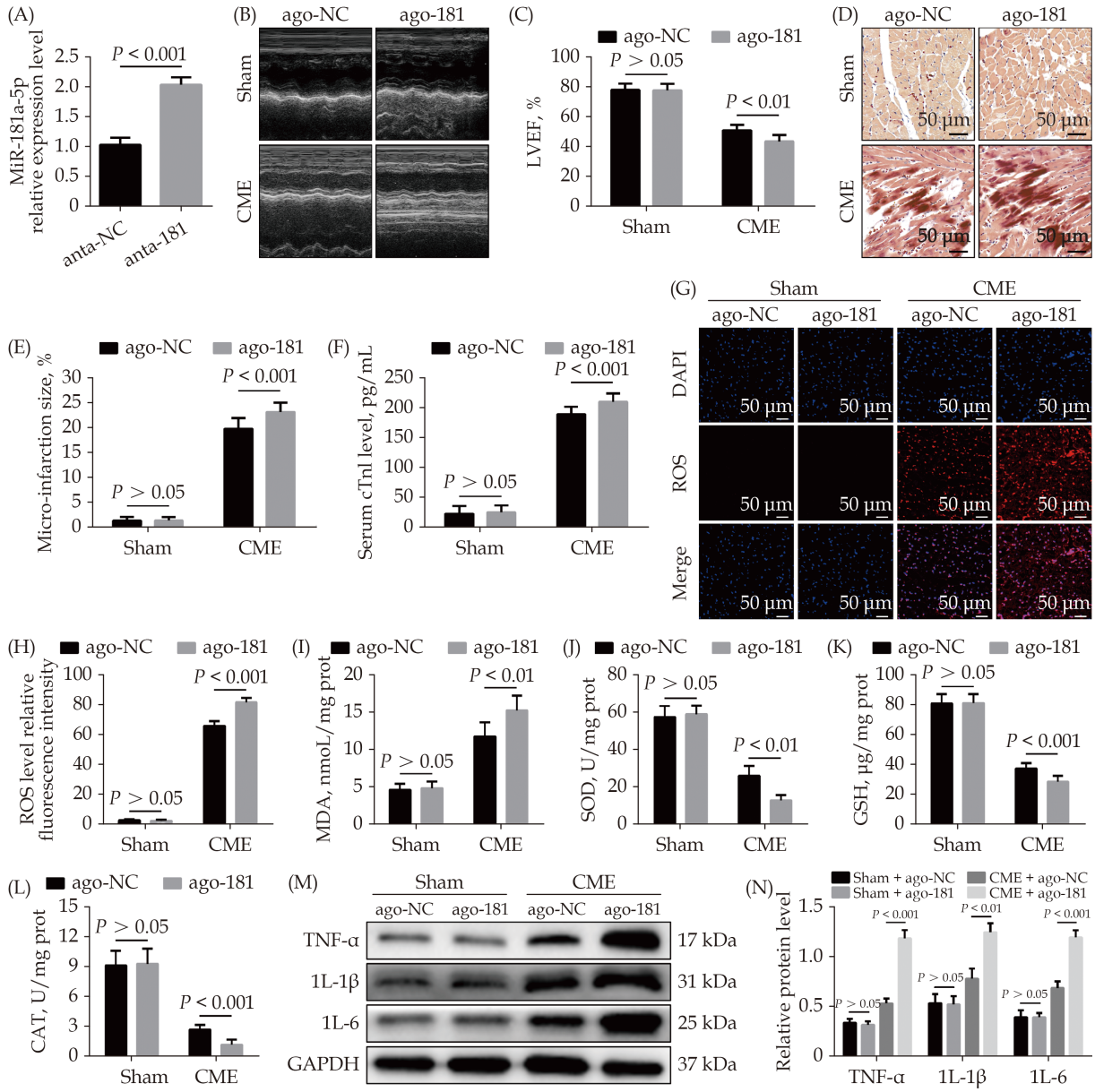

Figure 3 Overexpression of miR-181a-5p aggravates CME-induced myocardial oxidative stress and inflammatory injury. (A): Transfection with miR-181a-5p antagomiR elevated myocardial miR-181a-5p level significantly; (B & C): echocardiography was used to assess cardiac function and to quantify LVEF (n = 10); (D & E): haematoxylin-basic fuchsin-picric acid staining was used to measure micro-infarction size (× 200 magnification, scale bar = 50 μm) (n = 6); (F): serum cTnI concentration in each group (n = 10); (G & H): the ROS production was detected by the dichloro-dihydro-fluorescein diacetate assay (× 200 magnification, scale bar = 50 μm) (n = 6); (I–L): myocardial MDA, SOD, GSH, and CAT level in each group (n = 6); and (M & N): western blotting was used to quantify myocardial TNF-α, IL-1β, and IL-6 protein level, with glyceraldehyde 3-phosphate dehydrogenase as a loading control (n = 3). Data were shown as mean ± SE (standard error) based on at least three independent experiments. CAT: catalase enzymes; CME: coronary microembolization; cTnI: cardiac troponin I; GSH: glutathione; IL-1β: interleukin-1β; IL-6: interleukin 6; LVEF: left ventricular ejection fraction; MDA: malondialdehyde; ROS: reactive oxygen species; SOD: superoxide dismutase; TNF-α: tumor necrosis factor-α.

GSH, and CAT level (Figure 5I–5K). Moreover, western blotting results showed a significant decrease in the levels of myocardial TNF-α, IL-1β, and IL-6 proteins in the CME + Ad-XIAP group than the CME + Ad-NC group (Figure 5L–5O). The underlined results revealed that overexpression of XIAP could improve CME-initiated myocardial oxidative stress and inflammatory injury.

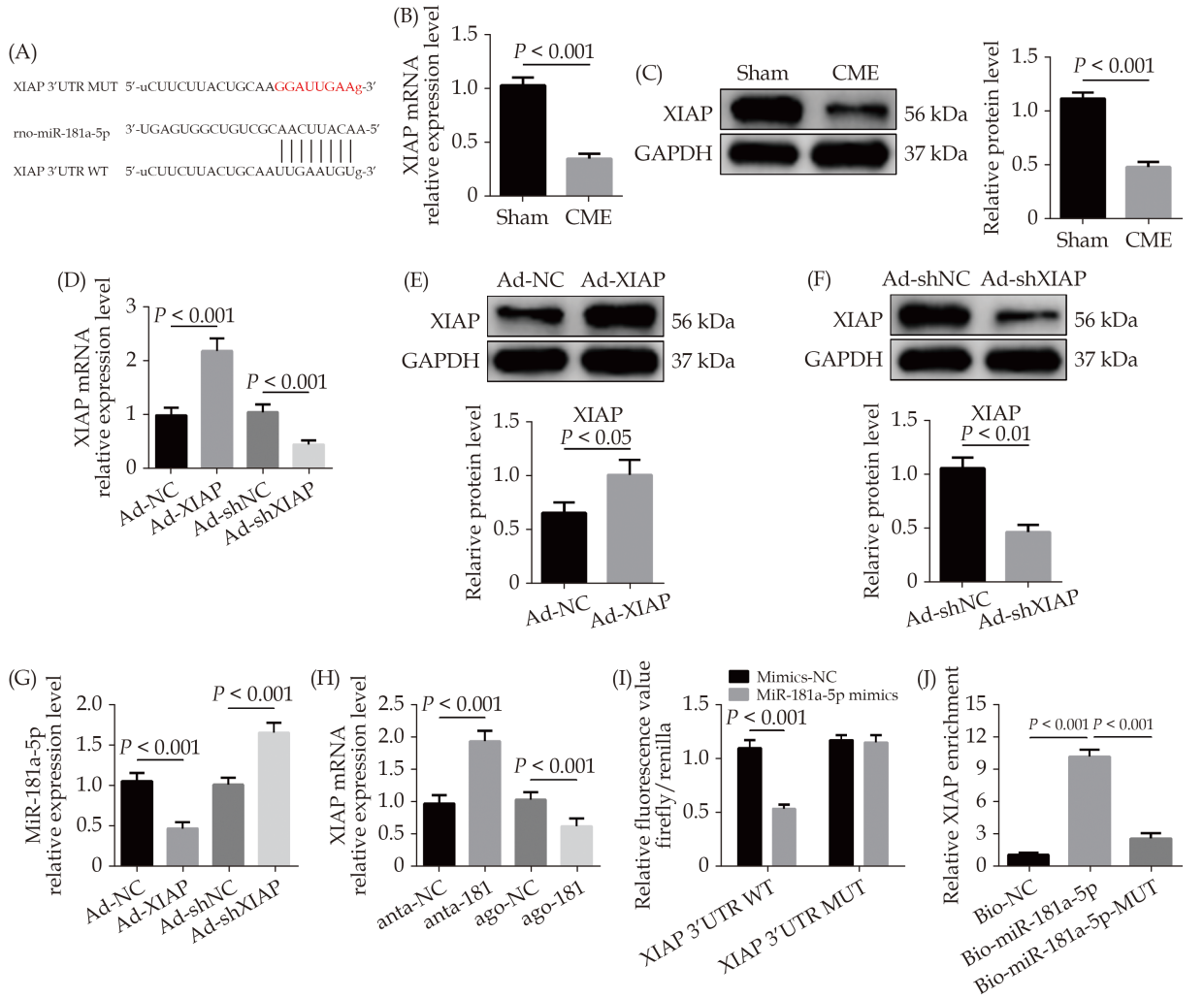

Figure 4 XIAP is a direct target of miR-181a-5p. (A): The predicted binding region between miR-181a-5p and XIAP mRNA was predicted by using bioinformatics analysis; (B): XIAP mRNA level was significantly decreased after CME (n = 10); (C): XIAP protein level was significantly decreased after CME (n = 3); (D): XIAP mRNA was overexpressed or silenced with Ad-XIAP or Ad-shXIAP, the qRT-PCR was used to detect the transfection efficiency (n = 10); (E): transfection with Ad-XIAP increased myocardial XIAP protein level significantly (n = 3); (F): transfection with Ad-shXIAP decreased myocardial XIAP protein level significantly (n = 3); (G): the expression level of miR-181a-5p was tested in XIAP-upregulated or XIAP-overexpressed rats with qRT-PCR (n = 10); (H): the expression levels of XIAP were tested in miR-181a-5p-downregulated or miR-181a-5p-overexpressed rats with qRT-PCR (n = 10); (I): relative luciferase activity in WT-XIAP and MUT-XIAP; and (J): RNA pulldown assay was applied to prove the binding relation between XIAP and miR-181a-5p. Data were shown as mean ± SE (standard error) based on at least three independent experiments. CME: coronary microembolization; MUT: mutant; qRT-PCR: quantitative reverse transcription polymerase chain reaction; TNF-α: tumor necrosis factor-α; WT: wild-type; XIAP: X-linked inhibitor of apoptosis protein.

Downregulation of MiR-181a-5p Attenuates Hypoxia-induced Oxidative Stress and Inflammatory Injury in Cardiomyocyte Through Regulation of XIAP

To study the underlying mechanism, we performed *in vitro* rescue experiments. When the miR-181a-5p expression was inhibited, the cell viability of H9c2 cells in hypoxia condition was significantly upregulated. Meanwhile, the LDH and cTnI level in supernatant were remarkably reduced. However, the inhibition of XIAP dramatically reversed these effects (Figure 6A–6C). The ROS and MDA level of cardiomyocytes were significantly reduced, but the SOD, GSH and CAT level were significantly increased in the Hypoxia + anta-181 group compared to the Hypoxia + anta-NC group, while XIAP knockdown dramatically reversed these effects (Figure 6D–6H).

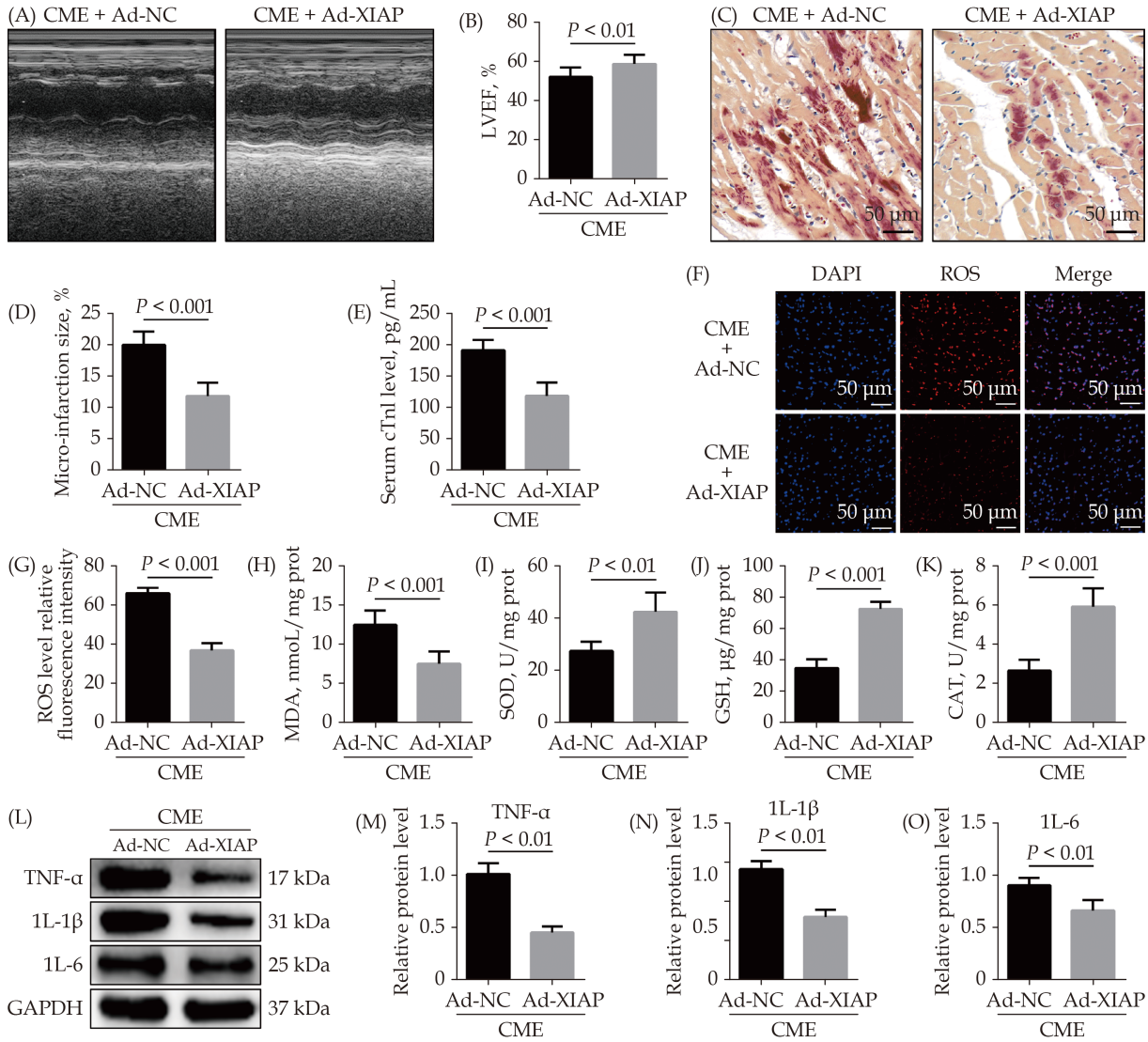

Figure 5 Overexpression of XIAP ameliorates CME-caused myocardial oxidative stress and inflammatory injury. (A & B): Echocardiography was used to assess cardiac function and to quantify LVEF (n = 10); (C & D): haematoxylin-basic fuchsin-picric acid staining was used to measure micro-infarction size (× 200 magnification, scale bar = 50 μm) (n = 6); (E): serum cTnI concentration in each group (n = 10); (F & G): the ROS production was detected by the dichloro-dihydro-fluorescein diacetate assay (× 200 magnification, scale bar = 50 μm) (n = 6); (H–K): myocardial MDA, SOD, GSH, and CAT level in each group (n = 6); and (L–O): western blotting was used to quantify myocardial TNF-α, IL-1β, and IL-6 protein level, with glyceraldehyde 3-phosphate dehydrogenase as a loading control (n = 3). Data were shown as mean ± SE (standard error) based on at least three independent experiments. CAT: catalase enzymes; CME: coronary microembolization; cTnI: cardiac troponin I; GSH: glutathione; IL-1β: interleukin-1β; IL-6: interleukin 6; LVEF: left ventricular ejection fraction; MDA: malondialdehyde; ROS: reactive oxygen species; SOD: superoxide dismutase; TNF-α: tumor necrosis factor-α; XIAP: X-linked inhibitor of apoptosis protein.

The results of immunoblotting revealed that treatment with miR-181a-5p antagomiR increased XIAP protein level in cardiomyocyte, and treatment with shXIAP decreased XIAP protein level. Expression level of TNF-α, IL-1β, and IL-6 proteins were dramatically downregulated by inhibition of miR-181a-5p, which were remarkably abolished by co-transfection with shXIAP (Figure 6I–6M). The underlined results indicated that the inhibition of miR-181a-5p could decrease the hypoxia-initiated cardiomyocyte oxidative stress and inflammatory injury, and the process through targeting XIAP.

DISCUSSION

CME is generally considered a spontaneous event

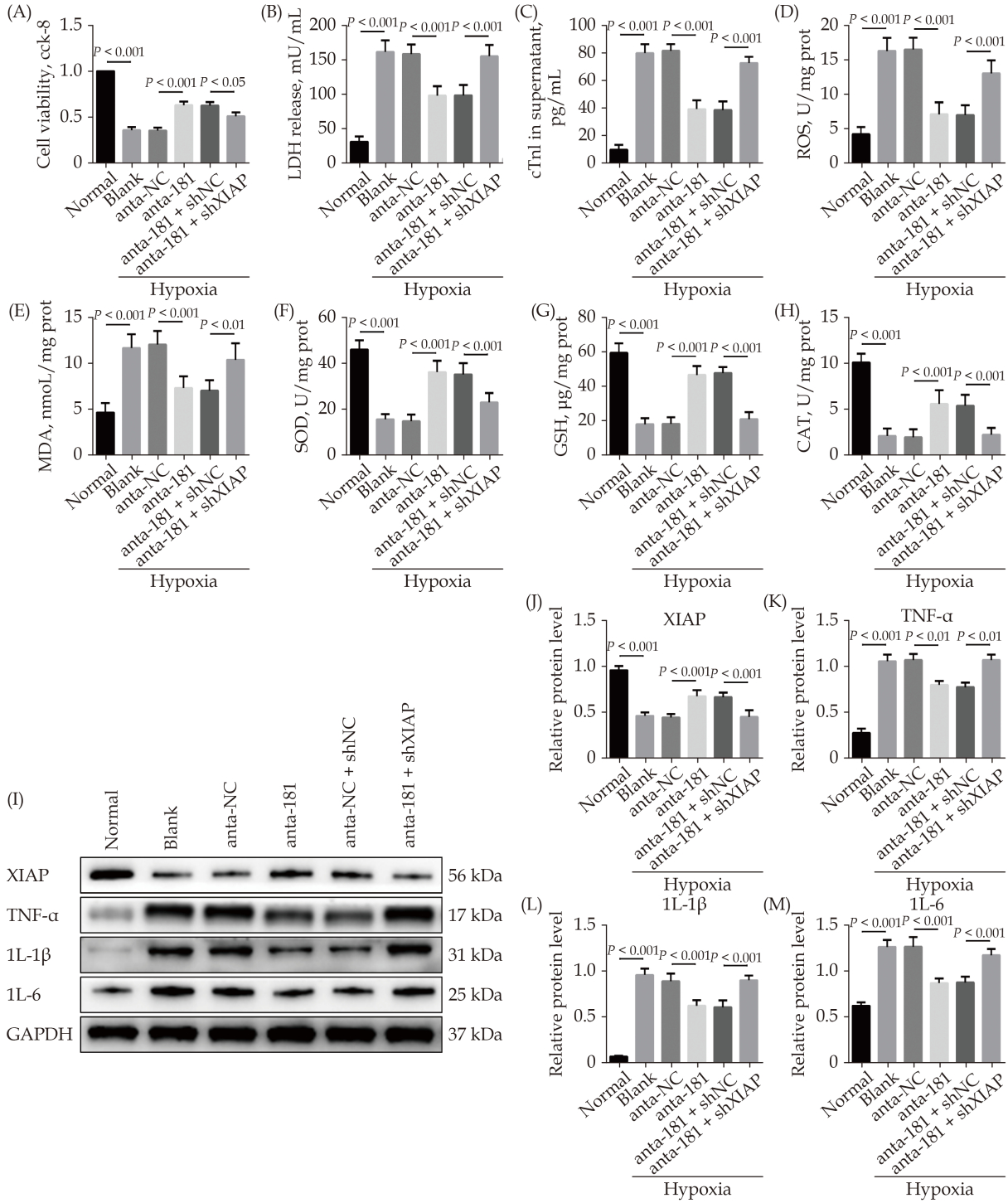

Figure 6 Downregulation of miR-181a-5p attenuates hypoxia-induced oxidative stress and inflammatory injury in cardiomyocyte through regulation of XIAP. (A): A CCK-8 assay used to gauge H9c2 cardiomyocyte viability (n = 3); (B & C): supernatant LDH and cTnI levels were measured via enzyme-linked immunosorbent assay (n = 6); (D–H): the ROS, MDA, SOD, GSH, and CAT levels in cardiomyocyte were detected (n = 6); and (I–M): western blotting was used to quantify cardiomyocyte XIAP, TNF-α, IL-1β, and IL-6 protein level, with glyceraldehyde 3-phosphate dehydrogenase as a loading control (n = 3). Data were shown as mean ± SE (standard error) based on at least three independent experiments. CAT: catalase enzymes; CCK-8: cell counting kit-8; cTnI: cardiac troponin I; GSH: glutathione; IL-1β: interleukin-1β; IL-6: interleukin 6; LDH: lactate dehydrogenase; MDA: malondialdehyde; ROS: reactive oxygen species; SOD: superoxide dismutase; TNF-α: tumor necrosis factor-α; XIAP: X-linked inhibitor of apoptosis protein.

in ischemic heart disease, or an iatrogenic complication of PCI.[22] Clinical and basic research have demonstrated that the degree of abnormal left ventricular systolic function caused by CME does not match the degree of blood flow disorder.[23] Dörge, *et al*.[24] also found that cardiac function was progressively impaired, but the total infarct size of myocardial tissue is less than 5%, which cannot fully explain the progressive cardiac dysfunction. In addition to reduced blood flow, there must be other reasons leading to myocardial damage following CME. The existing evidence has demonstrated that myocardial inflammatory response plays a crucial role in CME-caused myocardial damage. Li, *et al*.[25] found that inhibition of NF-κB pathway alleviated myocardial inflammatory response and cardiac dysfunction after coronary microembolization in rats. Another study discovered that blockade of TNF-α contributed to improve cardiac dysfunction after coronary microembolization in mini-pigs.[9] Our previous study has proved that pro-inflammatory cytokines, such as TNF-α, IL-1β and IL-6, play a major role in CME-induced myocardial damage.[26] Additionally, Su, *et al*.[11] reported that suppressing oxidative stress improves CME-induced cardiac dysfunction and alleviates myocardial damage, which indicating that oxidative stress also participates in CME-induced myocardial damage. In the present study, we found that the expression level of pro-inflammatory cytokines (TNF-α, L-1β and IL-6) and oxidative stress parameters (ROS and MDA) in heart tissue were significantly elevated after CME, whereas the level of anti-oxidative stress parameters (SOD, GSH and CAT) in heart tissue were dramatically decreased. All these results consistent with previous studies.[11,18,26]

The miRNA is a small molecule non-coding RNAs of about 21−25 nucleotides in length, and about one-third of all human genes are regulated by these RNAs.[27] It is well known that miRNAs specifically bind to target gene mRNA target mRNA 3′ untranslated region and participate in the regulation of many important life activities, thereby inhibiting protein synthesis at the post-transcriptional level.[28] MiRNAs play crucial roles in various physiological and pathological processes. The association between miRNAs and CME-induced myocardial damage has received increasing attention in recent years. MiR-142-3p is remarkedly downregulated in CME heart tissue, and overexpression of miR-142-3p alleviates CME-induced inflammatory injury by directly targeting IRAK-1.[18] Kong, *et al*.[29] reported that overexpression of miR-26a-5p improves cardiac function and reduces myocardial inflammation induced by CME through directly inhibiting HMGA1. Our previous study has found that miR-486-5p targeting PTEN protects against CME-induced myocardial injury.[19] However, research in this area is only beginning to emerge and deserves careful observation. In this study, we first time reported that miR-181a-5p is upregulated significantly in heart tissue undergoing CME. Inhibition of myocardial miR-181a-5p improves CME-induced cardiac dysfunction and alleviates CME-induced myocardial oxidative stress and inflammation, whereas overexpression of miR-181a-5p exerts the opposite effects. *In vitro* experiments also indicated that miR-181a-5p knockdown alleviates hypoxia-induced cardiomyocytes oxidative stress and inflammatory injury. Finally, bioinformatics analysis, DLR assay and RNA pulldown assay confirmed that XIAP is a direct target gene of miR-181a-5p.

XIAP, one of the inhibitors of apoptosis family members, has been confirmed as an important regulator of cell apoptosis.[30] Emerging studies have shown that XIAP can inhibit oxidative stress and inflammatory injury.[31,32] As reported in the literature, overexpression of XIAP inhibits oxidative stress in hypoxia/reoxygenation-treated cardiomyocytes.[32] Zhao, *et al*.[33] found that overexpression of XIAP protects against cadmium induction of ROS-dependent neuronal injury. Zilu, *et al*.[34] found that the reduction of XIAP suppresses NLRP3 inflammasome activation. Our previous study found that myocardial XIAP level is decreased after CME, and upregulated XIAP ameliorates CME-induced myocardial injury and apoptosis.[35] However, the role and mechanism of XIAP in CME-mediated cardiac oxidative stress and inflammatory injury is still unclear. Herein, we found that XIAP level was decreased significantly in CME heart tissue. Next, overexpression of XIAP partially rescued rats from CME-caused myocardial oxidative stress and inflammatory injury. *In vitro* rescue experiments revealed that downregulation of XIAP could abolish the protective effects of miR-181a-5p knockdown on hypoxia-induced cardiomyocyte oxidative stress and inflammatory injury.

LIMITATIONS

There are several mentionable limitations to the present study. On the one hand, while the rat CME model used for this analysis is widely used in the study of CME, it is still not a perfect clinical mimic of CME. It is thus necessary that models which more closely resemble clinical CME be developed. On the other hand, the mechanism underlying the process that miRNAs regulate cardiovascular diseases is complex. In the future, we may attempt to further investigate the related mechanisms of miRNAs on CME-induced cardiac repair.

CONCLUSIONS

In conclusion, depression of miR-181a-5p alleviates oxidative stress and inflammation by directly targeting XIAP in CME-caused myocardial damage. The miR-181a-5p/XIAP axis might act as a potential and novel therapeutic target for CME-induced myocardial injury.

ACKNOWLEDGMENTS

This study was supported by the National Natural Science Foundation of China (No.81770346), and the Project for Innovative Research Team in Guangxi Natural Science Foundation (2018GXNSFGA281006). All authors had no conflicts of interest to disclose.

REFERENCES

[1] Erbel R, Heusch G. Coronary microembolization. *J Am Coll Cardiol* 2000; 36: 22–24.
[2] Salem SA, Haji S, Garg N, *et al*. Occlusion of right coronary artery by microembolization caused by excessive diagnostic catheter manipulation. *Ann Transl Med* 2018; 6: 20.
[3] Heusch G, Skyschally A, Kleinbongard P. Coronary microembolization and microvascular dysfunction. *Int J Cardiol* 2018; 258: 17–23.
[4] Wang Y, Zhao HW, Wang CF, *et al*. Incidence, predictors, and prognosis of coronary slow-flow and no-reflow phenomenon in patients with chronic total occlusion who underwent percutaneous coronary intervention. *Ther Clin Risk Manag* 2020; 16: 95–101.
[5] Kalyoncuoglu M, Biter Hİ, Ozturk S, *et al*. Predictive accuracy of lymphocyte-to-monocyte ratio and monocyte-to-high-density-lipoprotein-cholesterol ratio in determining the slow flow/no-reflow phenomenon in patients with non-ST-elevated myocardial infarction. *Coron Artery Dis* 2020; 31: 518–526.
[6] Camici PG, Crea F. Coronary microvascular dysfunction. *N Engl J Med* 2007; 356: 830–840.
[7] Nakanishi K, Daimon M. Coronary slow flow and subclinical left ventricular dysfunction. *Int Heart J* 2019; 60: 495–496.
[8] Heusch G. The regional myocardial flow-function relationship: a framework for an understanding of acute ischemia, hibernation, stunning and coronary microembolization. 1980. *Circ Res* 2013; 112: 1535–1537.
[9] Chen ZW, Qian JY, Ma JY, *et al*. TNF-α-induced cardiomyocyte apoptosis contributes to cardiac dysfunction after coronary microembolization in mini-pigs. *J Cell Mol Med* 2014; 18: 1953–1963.
[10] Chen A, Chen Z, Zhou Y, *et al*. Rosuvastatin protects against coronary microembolization-induced cardiac injury via inhibiting NLRP3 inflammasome activation. *Cell Death Dis* 2021; 12: 78.
[11] Su Q, Lv X, Ye Z. Ligustrazine attenuates myocardial injury induced by coronary microembolization in rats by activating the PI3K/Akt pathway. *Oxid Med Cell Longev* 2019; 2019: 6791457.
[12] Zhu L, Li N, Sun L, *et al*. Non-coding RNAs: the key detectors and regulators in cardiovascular disease. *Genomics* 2021; 113: 1233–1246.
[13] Arabian M, Mirzadeh Azad F, Maleki M, *et al*. Insights into role of microRNAs in cardiac development, cardiac diseases, and developing novel therapies. *Iran J Basic Med Sci* 2020; 23: 961–969.
[14] Zhou H, Ni WJ, Meng XM, *et al*. MicroRNAs as regulators of immune and inflammatory responses: potential therapeutic targets in diabetic nephropathy. *Front Cell Dev Biol* 2021; 8: 618536.
[15] Colpaert RMW, Calore M. Epigenetics and microRNAs in cardiovascular diseases. *Genomics* 2021; 113: 540–551.
[16] Ye H, Xu G, Zhang D, *et al*. The protective effects of the miR-129-5p/keap-1/Nrf2 axis on Ang II-induced cardiomyocyte hypertrophy. *Ann Transl Med* 2021; 9: 154.
[17] Qu Y, Zhang J, Zhang J, *et al*. MiR-708-3p alleviates inflammation and myocardial injury after myocardial infarction by suppressing ADAM17 expression. Inflammation. Published Online First: 25 January 2021. DOI: 10.1007/s10753-020-01404-9.
[18] Su Q, Lv X, Ye Z, *et al*. The mechanism of miR-142-3p in coronary microembolization-induced myocardiac injury via regulating target gene IRAK-1. *Cell Death Dis* 2019; 10: 61.
[19] Zhu HH, Wang XT, Sun YH, *et al*. MicroRNA-486-5p targeting PTEN protects against coronary microembolization-induced cardiomyocyte apoptosis in rats by activating the PI3K/AKT pathway. *Eur J Pharmacol* 2019; 855: 244–251.
[20] Sun X, Sit A, Feinberg MW. Role of miR-181 family in regulating vascular inflammation and immunity. *Trends Cardiovasc Med* 2014; 24: 105–112.
[21] Sun YH, Su Q, Li L, *et al*. Expression of p53 in myocardium following coronary microembolization in rats and its significance. *J Geriatr Cardiol* 2017; 14: 292–300.
[22] Heusch G. The coronary circulation as a target of cardioprotection. *Circ Res* 2016; 118: 1643–1658.
[23] Malyar NM, Lerman LO, Gössl M, *et al*. Relation of nonperfused myocardial volume and surface area to left ventricular performance in coronary microembolization. *Circulation* 2004; 110: 1946–1952.

[24] Dörge H, Schulz R, Belosjorow S, *et al*. Coronary microembolization: the role of TNF-alpha in contractile dysfunction. *J Mol Cell Cardiol* 2002; 34: 51−62.
[25] Li S, Zhong S, Zeng K, *et al*. Blockade of NF-kappaB by pyrrolidine dithiocarbamate attenuates myocardial inflammatory response and ventricular dysfunction following coronary microembolization induced by homologous microthrombi in rats. *Basic Res Cardiol* 2010; 105: 139−150.
[26] Su Q, Li L, Sun Y, *et al*. Effects of the TLR4/Myd88/NF-kappaB signaling pathway on NLRP3 inflammasome in coronary microembolization-induced myocardial injury. *Cell Physiol Biochem* 2018; 47: 1497−1508.
[27] Ambros V. MicroRNAs: tiny regulators with great potential. *Cell* 2001; 107: 823−826.
[28] Ke XS, Liu CM, Liu DP, *et al*. MicroRNAs: key participants in gene regulatory networks. *Curr Opin Chem Biol* 2003; 7: 516−523.
[29] Kong B, Qin Z, Ye Z, *et al*. MicroRNA-26a-5p affects myocardial injury induced by coronary microembolization by modulating HMGA1. *J Cell Biochem* 2019; 120: 10756−10766.
[30] Qin S, Yang C, Zhang B, *et al*. XIAP inhibits mature Smac-induced apoptosis by degrading it through ubiquitination in NSCLC. *Int J Oncol* 2016; 49: 1289−1296.
[31] Estornes Y, Bertrand MJM. IAPs, regulators of innate immunity and inflammation. *Semin Cell Dev Biol* 2015; 39: 106−114.
[32] Lu M, Qin X, Yao J, *et al*. MiR-134-5p targeting XIAP modulates oxidative stress and apoptosis in cardiomyocytes under hypoxia/reperfusion-induced injury. *IUBMB Life* 2020; 72: 2154−2166.
[33] Zhao R, Yu Q, Hou L, *et al*. Cadmium induces mitochondrial ROS inactivation of XIAP pathway leading to apoptosis in neuronal cells. *Int J Biochem Cell Biol* 2020; 121: 105715.
[34] Zilu S, Qian H, Haibin W, *et al*. Effects of XIAP on high fat diet-induced hepatic steatosis: a mechanism involving NLRP3 inflammasome and oxidative stress. *Aging* 2019; 11: 12177−12201.
[35] Zheng J, Long M, Qin Z, *et al*. Nicorandil inhibits cardiomyocyte apoptosis and improves cardiac function by suppressing the HtrA2/XIAP/PARP signaling after coronary microembolization in rats. *Pharmacol Res Perspect* 2021; 9: e00699.

Please cite this article as: ZHOU Y, LONG MY, CHEN ZQ, HUANG JW, QIN ZB, LI L. Downregulation of miR-181a-5p alleviates oxidative stress and inflammation in coronary microembolization-induced myocardial damage by directly targeting XIAP. *J Geriatr Cardiol* 2021; 18(6): 426−439. DOI: 10.11909/j.issn.1671-5411.2021.06.007